

**Test Results of 15 T Nb<sub>3</sub>Sn Quadrupole Magnet HQ01 with a 120 mm Bore for the  
LHC Luminosity Upgrade**

**S. Caspi, B. Bingham, D. Cheng, D. R. Dietderich, H. Felice, P. Ferracin, R. Hafalia,  
R. Hannaford, J. Joseph, G. L. Sabbi and X. Wang**

Lawrence Berkeley National Laboratory, 1 Cyclotron Road, Berkeley CA 94720

**G. Ambrosio, E. Barzi, R. Bossert, G. Chlachidze, V. V. Kashikhim, and A. V.  
Zlobin**

Fermilab National Laboratory, Batavia, IL 60510

**M. Anerall, A. Ghosh, J. Schmalzle, J. Schmalzle and P. Wanderer**

Brookhaven National Laboratory, Upton, NY 11973-5000

**DISCLAIMER**

This document was prepared as an account of work sponsored by the United States Government. While this document is believed to contain correct information, neither the United States Government nor any agency thereof, nor The Regents of the University of California, nor any of their employees, makes any warranty, express or implied, or assumes any legal responsibility for the accuracy, completeness, or usefulness of any information, apparatus, product, or process disclosed, or represents that its use would not infringe privately owned rights. Reference herein to any specific commercial product, process, or service by its trade name, trademark, manufacturer, or otherwise, does not necessarily constitute or imply its endorsement, recommendation, or favoring by the United States Government or any agency thereof, or The Regents of the University of California. The views and opinions of authors expressed herein do not necessarily state or reflect those of the United States Government or any agency thereof or The Regents of the University of California.

This work was supported by the Director, Office of Science, Office of Fusion Energy Sciences, of the U.S. Department of Energy under Contract No. DE-AC02-05CH11231.

# Test Results of 15 T Nb<sub>3</sub>Sn Quadrupole Magnet HQ01 with a 120 mm Bore for the LHC Luminosity Upgrade

S. Caspi, G. Ambrosio, M. Anerella, E. Barzi, B. Bingham, R. Bossert, D. W. Cheng, G. Chlachidze, D. R. Dietderich, H. Felice, P. Ferracin, A. Ghosh, A. R. Hafalia, C. R. Hannaford, J. Joseph, V. V. Kashikhin, G. L. Sabbi, J. Schmalzle, P. Wanderer, W. Xiaorong, and A. V. Zlobin

**Abstract**—In support of the luminosity upgrade of the Large Hadron Collider (LHC), the US LHC Accelerator Research Program (LARP) has been developing a 1-meter long, 120 mm bore Nb<sub>3</sub>Sn IR quadrupole magnet (HQ). With a short sample gradient of 219 T/m at 1.9 K and a conductor peak field of 15 T, the magnet will operate under higher forces and stored-energy levels than that of any previous LARP magnet models. In addition, HQ has been designed to incorporate accelerator quality features such as precise coil alignment and adequate cooling. The first 6 coils (out of the 8 fabricated so far) have been assembled and used in two separate tests—HQ01a and HQ01b. This paper presents design parameters, summary of the assemblies, the mechanical behavior as well as the performance of HQ01a and HQ01b.

**Index Terms**—HQ, LARP, Nb<sub>3</sub>Sn, phase-II, superconducting quadrupole magnet.

## I. INTRODUCTION

DESPITE the complexity of its processing technology, compared to NbTi, Nb<sub>3</sub>Sn remains the most feasible choice for future high field accelerator magnets. Three US laboratories (BNL, FNAL, and LBNL), collaborating within the LARP program, are employing Nb<sub>3</sub>Sn technology in a magnet design that will present a full scale IR quadrupole magnet option for the LHC luminosity upgrade (proposed to be installed 2020-2021) [1], [2]. In 2004, LARP started developing a 1 m long IR quadrupole (TQ) that reached 200 T/m in a 90 mm aperture [3], [4]. That program demonstrated that the 200 T/m target gradient could be consistently achieved and exceeded. TQ reached a peak gradient of 237 T/m at 1.9K and current plateaus above 90% of “short-sample” [5]. The collaboration extended the 1 m long TQ technology to a 3.6 m magnet (LQ) [6]–[8]. In on-going tests, LQ is demonstrating similar performance as TQ [9], [10].

Manuscript received August 03, 2010; accepted October 07, 2010 Date of publication November 09, 2010; date of current version May 27, 2011. This work was supported in part by the Director, Office of Science, High Energy Physics, U.S. Department of Energy under Contract DE-AC02-05CH11231 and in part by the DOE through the US LHC Accelerator Research Program.

S. Caspi, B. Bingham, D. Cheng, D. R. Dietderich, H. Felice, P. Ferracin, R. Hafalia, R. Hannaford, J. Joseph, G. L. Sabbi, and W. Xiaorong are with the Lawrence Berkeley National Laboratory, Berkeley, CA 94720 USA (e-mail: s\_caspi@lbl.gov).

G. Ambrosio, E. Barzi, R. Bossert, G. Chlachidze, V. V. Kashikhin, and A. Zlobin are with the Fermi National Laboratory, Batavia, IL 60510-0500 USA.

M. Anerella, A. Ghosh, J. Schmalzle, and P. Wanderer are with the Brookhaven National Laboratory, Upton, NY 11973-5000 USA.

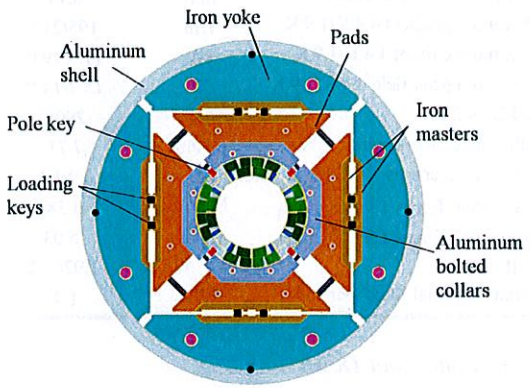


Fig. 1. HQ cross-section—120 mm high gradient Nb<sub>3</sub>Sn quadrupole.

To meet CERN’s upgrade requirements, LARP is also developing a new, high-gradient IR quadrupole magnet, HQ, with an increased bore size of 120 mm which will push the field in the conductor to 15 T. This magnet will include features such as coil alignment and field quality and will operate at a gradient above CERN’s original upgrade of 120 T/m using NbTi conductor [11], [12]. This paper summarizes the design parameters and reports the results of two tests HQ01a and HQ01b.

## II. MAGNET DESIGN

### A. HQ—Conceptual Design and Parameters

The cross-section of the HQ quadrupole is shown in Fig. 1. The magnet components include:  $\cos 2\theta$  coils, collars, pads, yokes and an outer shell. The effectiveness of the structural components was previously tested as part of the LARP TQ program with the exception of the collars [13], [14]. The aluminum collars are incorporated into the design to provide alignment and assembly control but not for pre-stress [15]. Aluminum was picked as a high thermal contraction material to reduce the pre-stress it intercepts during cool-down.

The double layer coil uses 35 strands Rutherford cable insulated with an S2 glass sleeve. 54/61 and 108/127 filament cables are used made with Nb<sub>3</sub>Sn RRP 0.8 mm strands. Each of the two layers of the coil is wound around titanium alloy poles (islands) and includes stainless steel end-shoes and spacers. A single aluminum-bronze wedge, within each octant, separates each layer into two blocks. The overall design parameters are listed in Table I.

TABLE I  
HQ01 PARAMETERS

Coil aperture	mm	120
Yoke OR	mm	260
Outer Shell thickness	mm	25
Overall magnet diameter	mm	570
Bare cable width	mm	15.11
Bare cable mid-thickness	mm	1.44
Cable keystone angle	deg	0.75
Cable insulation thickness	mm	0.09
Turns per quadrant IL/OL		20/26
Mid-plane shim per octant	mm	0.14
Maximum gradient 4.4 K/1.9 K	T/m	195/214
Maximum current 4.4 K/1.9 K	kA	17.3/19.0
Maximum peak field 4.4 K/1.9 K	T	13.7/14.9
$J_c$ 12T, 4.2 K	A/mm <sup>2</sup>	2900
Inductance (at quench)	mH/m	7.71
Max. stored energy 4.4K/1.9 K	MJ	0.9/1.1
Max octant forces 1.9 K Fx total	MN/m	3.38
Max octant forces 1.9 K Fy total	MN/m	-5.03
$F_\theta$ IL/OL	MN/m	-1.92/-3.2
Maximum axial force per end	MN	1.4

### B. Assembly and Cool-Down

The coil-pack subassembly consists of four aluminum collar quadrants that are bolted around the coils. Each coil has an alignment key engaging a longitudinal keyway in the coil's outer layer island (Fig. 1). The collar quadrants clamp on the pole (alignment) keys as they are bolted together. The collars are used for assembly and alignment only, and do not provide pre-stress as traditionally done in NbTi magnets. Surrounding the faceted collars are four steel pads with matching facets. The pad-quadrants are lightly bolted to each other—completing the coil pack subassembly. A separate subassembly, the shell-yoke structure, is composed of laminated iron yoke quadrants and an aluminum shell. The shell and yoke quadrants are locked together, following a bladder operation that stretches the shell, with interference “yoke gap-keys” between the yoke quadrants—locking and preloading the subassembly. During this operation, alignment pins are inserted in precision-machined alignment grooves between the yokes and the shell inner surface in four places.

During the final assembly, the coil-pack assembly is inserted into the shell-yoke structure on faceted “master keys” (alignment components) which engage matching profiles in both coil-pack and yoke structures. Bladders and interference load keys (Fig. 1) are inserted between the master keys. Bladder pressurization operations are performed to, outwardly, push the yokes (further stretching the shell) and, inwardly, compress the coil-pack. Once the target azimuthal strain on the instrumented shell is attained, the load keys are interference shimmed. The bladders are, then, deflated and removed along with the yoke gap keys, collapsing and locking the shell-yoke structure onto the keys and coil pack. The tension in the outer aluminum shell is now balanced by the azimuthal compressive stress in the coils. The final coil pre-stress is attained during cool-down as the aluminum shrinks over the yoke and pads due to the thermal expansion differences between the two.

TABLE II  
AVERAGE AZIMUTHAL STRESS

Location	$\sigma_\theta$ RT (MPa)	$\sigma_\theta$ 4K (MPa)	$\sigma_\theta$ Ex (MPa)
Layer 1 Island	-68	-160	+54
Layer 2 Island	-23	-49	+33
Layer 1 pole-turn	-48	-140	-7
Layer 2 pole-turn	-24	-78	+9
Outer Shell	+100	+210	+214

TABLE III  
AVERAGE AXIAL STRESS

Location	$\sigma_z$ RT (MPa)	$\sigma_z$ 4K (MPa)	$\sigma_z$ Ex (MPa)
Layer 1 Island	-18	-163	-90
Layer 2 Island	-6	-128	-91
Layer 1 pole-turn	-10	+18	+50
Layer 2 pole-turn	-5	+30	+53
Outer Shell	+25	+67	+70
Axial Rods ( $\sigma_z$ )	+93	+191	+205

### C. Mechanical Analysis

2D and 3D Finite Element Analyses were performed with ANSYS to determine the target stresses in the windings and structure. The analyses were done in 3 load cases—a) during room temperature loading (“bladder operation RT”), b) cool-down (“4K”) and c) excitation (“Ex”). Tables II and III summarize the average stress in the coil-island, coil pole turn, shell and axial rods from assembly to “short-sample limit”. A maximum local stress of 209 MPa was predicted after cool-down in layer 1 third turn from the island. Such a local high stress was previously predicted in TQ with minimum impact on its performance. HQ instrumentation and coil protection heaters are described in [16], [17]. An alternative design of the structure with features that address installation in a facility is described in [18].

## III. TEST RESULTS

Two magnet tests were performed. The first test, HQ01a, was done with the first four coils built for the HQ—coils #1, #2, #3, #4. The second test, HQ01b, replaced two of the HQ01a coils #2 and #3 with new coils, #5 and #6. The results of both tests are given below.

### A. HQ01a Assembly and Test

Although no practice coils were made (except for several winding tests with Rapid Prototype components), the quality of the first four coils was sufficient to justify a mechanical cool-down test. It was later decided to proceed and energize the magnet as well.

During the coil pack assembly, the aluminum collars came close to the alignment keys but did not make contact—gaps of 150 micron were measured on both sides of the alignment keys. From the analyses, it was evident, that even during cool-down the gaps did not close. Fig. 2 shows measured azimuthal and axial stress values at various steps during the test: a) initial azimuthal and axial loading (T+Z), b) final azimuthal loading (T), c) after cool-down to 4.4 K d) before warm-up, and e) after warm up.

The azimuthal and axial stress of the coils was monitored by strain gages mounted on each coil's layer 1 island. Although the structure followed design expectation, the pre-stress gain during

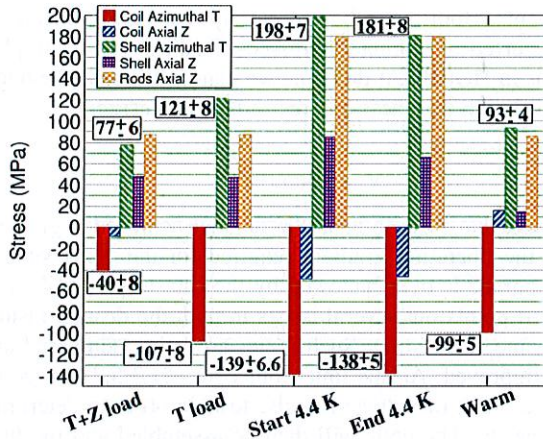


Fig. 2. Measured stress during various steps of HQ01a test.

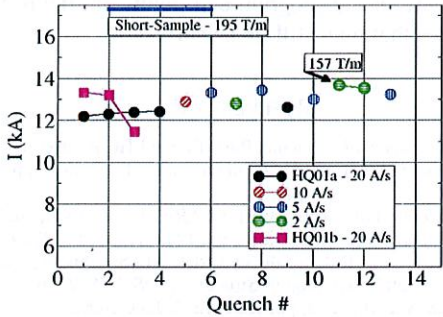


Fig. 3. HQ01a training curve.

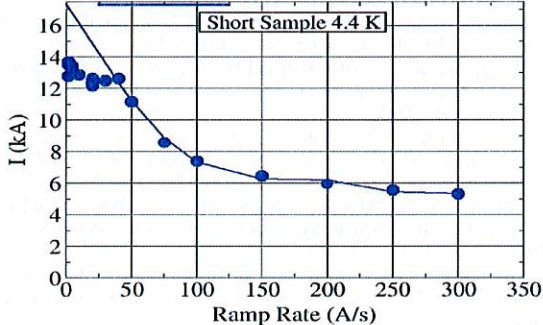


Fig. 4. HQ01a ramp rate dependence.

cool-down was insufficient and a correction was later applied during the second test of HQ01b.

Fig. 3 summarizes the magnet training performance. The first training quench was at 12183A (140T/m, peak-field of 9.7T, 71% of short-sample) increasing to a maximum of 13683A after 11 quenches (157T/m, 10.8T peak-field and 79% of short-sample) with a ramp rate of 2A/s. The ramp-rate sensitivity is evident in Fig. 4. Based on the ramp-rate behavior and the fact that all quenches (below 40A/s) originated in coil #3, the HQ01a test was terminated.

### B. HQ01a Disassembly and Inspection

An inspection of the coils after disassembly did not show any visual faults in coil #3. However coil #2, which never quenched, showed signs of arcing-damage on the outer layer near the lead-

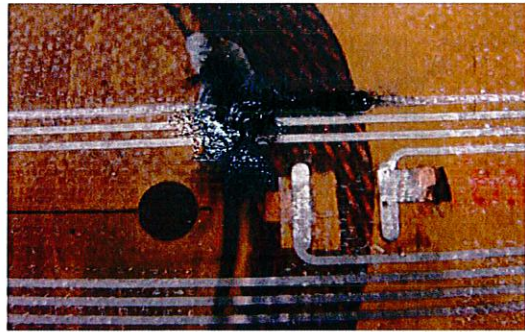


Fig. 5. Cracked epoxy across turns of the outer layer of coil #2 (HQ01a).

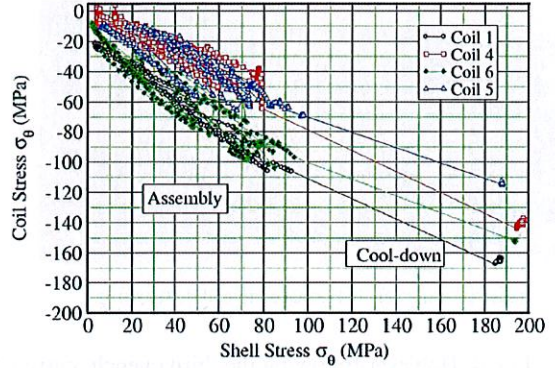


Fig. 6. Measured stress in coils and shell during assembly and cool-down.

end. A linear crack opened up in the epoxy along one of instrumentation trace-lines across the turns from the outer shoe to the spacer, Fig. 5. Upon further inspection using a Voltage Impulse Tester, activities of voltage breakdown could be seen—indicative of turn-to-turn and/or layer-to-layer arcing. Our plan remains to cut the coil apart for further inspection.

### C. HQ01b Assembly and Test

A second test was carried out after coils #2 and #3 were replaced with new coils #5 and #6. Several changes were introduced. First, a Fuji paper test was done to determine the contact uniformity between the coils and the aluminum collars. The test showed a symptom of an oversized coil profile—where coil-collar contact is concentrated near the pole (island) and lack of contact near the mid-plane. Increasing the radius of the collar by removing several sheets of the G10 ground-plane insulating laminations initially placed between the coils and the collars, improved the contact uniformity. The G10 thickness of all the quadrants was reduced from 0.9 mm to 0.25 mm. The same type of investigation and procedure was performed on the previous LQ magnet assemblies [10]. As a result the coil azimuthal compression versus the shell tension during assembly showed the expected linear behavior (Fig. 6). A second modification, with respect to HQ01a, was made to the size of the alignment keys. To ensure contact between collars and keys G10 shims were added to both sides of each key. The administered changes indicated an improvement in the applied pre-stress to the coils during cool-down.

The first quench of HQ01b was at 13308A (153T/m, 77% of short-sample) a gain of more than 1000 A with respect to

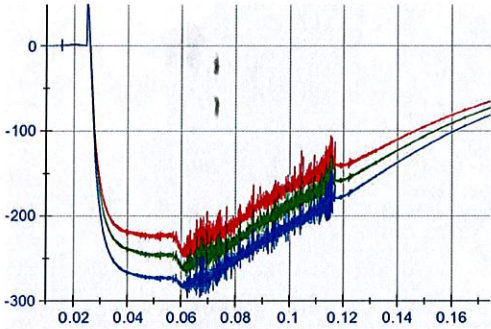


Fig. 7. Measured voltage on coil #6 following quench #1.

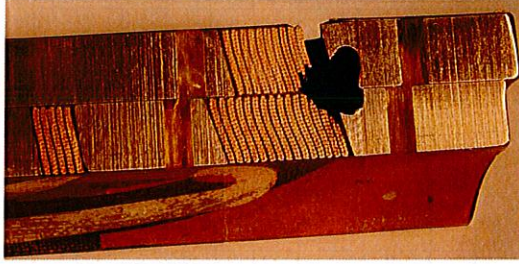


Fig. 8. Autopsy showing detailed damage to coil #6 (HQ01b).

HQ01a, Fig. 4. However following the third quench, current to the magnet could not be sustained and the test was terminated. It should be noted that during initial provoked quenches as well as during training the magnet voltage signals exhibited a behavior typical of arcing (Fig. 7). The decision to continue testing was based on: a) similar signals were also seen during the HQ01a test with no direct impact on its performance b) pushing the magnet to help and understand the problem.

#### D. HQ01b Disassembly and Inspection

As the magnet was being removed from the cryostat, it became evident that coil #6 suffered a major fault as a result of a voltage breakdown. A hole in the outer layer coil and shoe of coil #6 could be seen near the return-end. There was complete disintegration of two turns on the outer layer adjacent to the shoe. The autopsy showed major arc-damage between layers and a possible layer to layer short, Fig. 8.

#### IV. DISCUSSION

With a damaged lead-end of coil #2 and a damaged return-end of coil #6, it is clear that future HQ coils will be required to undergo more rigorous testing before assembly and a reexamination of the voltage levels applied during hi-pot. We are now performing additional voltage impulse tests on all coils. We note that such tests were not previously performed (or required) on any of the more than thirty five coils built for the TQ and LQ programs. Despite the similarity on many of details between the HQ and the TQ/LQ coils a closer look at the HQ-end suggests a potential weakness. The end block of layer 2 is nesting directly over the end block of layer 1 (Fig. 8). At the same time the end shoes of both layers and the coil-ends all meet together at the same spot forming a hazardous situation where any voltage-insulating breakdown may cause arcing to a number of different

components. Both tests showed clearly that insulation breakdown occurred and arcing progressed—leading to a catastrophic failure as in HQ01b. At this time we plan to increase the interlayer insulation thickness and revise the end design.

#### V. CONCLUSION

The fact that in both tests the magnet achieved a gradient beyond the operating gradient required for the NbTi version of the upgrade is overshadowed by the catastrophic failure of coil #6. It points out several issues in both the design, insulation scheme and testing. Such issues are being addressed and will be improved. At this time, four coils (#1,3,5,7) are going through a series of voltage impulse tests in order to determine their integrity. The coils will then be assembled and the final determining quality control test for voltage activity will be performed during provoked quenches. This incident is attributed to the R&D nature of the program and points out the difficulties and challenges that may still lie ahead.

#### REFERENCES

- [1] S. A. Gourlay *et al.*, "Magnet R&D for the LHC Accelerator Research Program," *IEEE Trans. Appl. Supercond.*, vol. 16, no. 2, pp. 324–327, June 2006.
- [2] P. Wanderer *et al.*, "Overview for LARP Magnet R&D," *IEEE Trans. Appl. Supercond.*, vol. 19, no. 3, pp. 1208–1211, June 2009.
- [3] S. Caspi *et al.*, "Test Results of LARP Nb<sub>3</sub>Sn Quadrupole Magnets Using a Shell-based Support Structure (TQS)," *IEEE Trans. Appl. Supercond.*, vol. 19, no. 3, pp. 1221–1225, June 2009.
- [4] B. Bossert *et al.*, "Fabrication and Test of LARP Technological Quadrupole Models of TQC Series," *IEEE Trans. Appl. Supercond.*, vol. 19, no. 3, pp. 1226–1230, June 2009.
- [5] H. Felice *et al.*, "Test results of TQS03: a LARP shell-based Nb<sub>3</sub>Sn quadrupole using 108/127 conductor," in *9th European Conf. on Appl. Supercond.*, Dresden, Germany, Sept. 2009, to be published.
- [6] P. Wanderer *et al.*, "Construction and Test of a 3.6 m Nb<sub>3</sub>Sn Racetrack Coils for LARP," *IEEE Trans. Appl. Supercond.*, vol. 18, no. 2, pp. 171–174, June 2008.
- [7] P. Ferracin *et al.*, "Fabrication and Test of a 3.7 m Long Support Structure for the LARP Nb<sub>3</sub>Sn Quadrupole Magnet LQS01," *IEEE Trans. Appl. Supercond.*, vol. 19, no. 3, pp. 1106–1111, June 2009.
- [8] G. Ambrosio *et al.*, "Development and Coil Fabrication for the LARP 3.7-m Long Nb<sub>3</sub>Sn Quadrupole," *IEEE Trans. Appl. Supercond.*, vol. 19, no. 3, pp. 1231–1234, June 2009.
- [9] G. Ambrosio *et al.*, "Test results of the first 3.7 m long Nb<sub>3</sub>Sn quadrupole by LARP and future plans," in *Paper ILX-05 this Conference*.
- [10] P. Ferracin *et al.*, "Mechanical performance of the LARP Nb<sub>3</sub>Sn quadrupole magnet LQS01," in *Paper 3LY-04 this Conference*.
- [11] R. Ostrojic, LHC Interaction Region Upgrade—Phase I LHC PR 1094, August 2008.
- [12] P. Fessia *et al.*, "Design of a 120 mm bore quadrupole for the LHC upgrade phase I," in *Paper IAO-04 this conference*.
- [13] S. Caspi *et al.*, "Mechanical Design of a Second Generation LHC IR Quadrupole," *IEEE Trans. Appl. Supercond.*, vol. 14, no. 2, pp. 235–238, June 2004.
- [14] A. R. Hafalia *et al.*, "Structure for an LHC 90 mm Nb<sub>3</sub>Sn quadrupole magnet," *IEEE Trans. Appl. Supercond.*, vol. 15, no. 2, pp. 1444–1447, June 2005.
- [15] H. Felice *et al.*, "Design of HQ-A High Field Large Bore Nb<sub>3</sub>Sn Quadrupole Magnet for LARP," *IEEE Trans. Appl. Supercond.*, vol. 19, no. 3, pp. 1235–1239, June 2009.
- [16] P. Bauer *et al.*, "Concept for a quench calculation program for the analysis of quench protection systems for superconducting high field magnets FNAL TD Notes TD-00-027.
- [17] H. Felice *et al.*, "Instrumentation and Quench Protection for LARP Nb<sub>3</sub>Sn Magnets," *IEEE Trans. Appl. Supercond.*, vol. 19, no. 3, pp. 2458–2462, June 2009.
- [18] M. Anerella *et al.*, "Alternative mechanical structure for LARP Nb<sub>3</sub>Sn quadrupoles," in *Paper 5LPH-01/200 this Conference*.